Scientific
Research
Publishing

Influence of Mg²⁺, Fe²⁺ and Zn²⁺ Cations on ¹³C-¹⁸O Bonds in Precipitated Aragonite, Calcite and Dolomite: An *ab Initio* Study

Jie Yuan

Key Laboratory of Earth and Planetary Physics, Institute of Geology and Geophysics, Chinese Academy of Science, Beijing, China
Email: yuanjie@mail.iggcas.ac.cn

Open Access

Abstract

The influence of metal cations on ¹³C-¹⁸O bonds in carbonates is still under debate. This paper used *ab initio* method to investigate this kind of influence of Mg²⁺, Fe²⁺ and Zn²⁺ cations on ¹³C-¹⁸O bonds in precipitated aragonite, calcite and dolomite. The polynomials of Δ_{47} and reduced partition function ratios (RPFRs) for ¹³/¹²C, ¹⁴/¹²C and ¹⁸/¹⁶O of these minerals were given within temperatures ranging from 260 to 1500 K. We found that these cations significantly decreased the Δ_{47} values at the level of 10^{-3} - 10^{-2} *per mil*, comparing with pure crystals; and that if the Δ_{47} values were used to reconstruct the temperatures *Ts*, the deviation of *T* was about 7.2°C for, for instance, zinc-enriched aragonite, as discussed in our paper. It was suggested that due to such influence, researchers would better use a proper thermometer according to the main impurity metal cations in carbonates. We also found that according to the probability theory, the theoretical value of the influence of phosphoric acid on Δ_{47} of CO_2 degassed from different carbonates was zero.

Keywords

1. Introduction

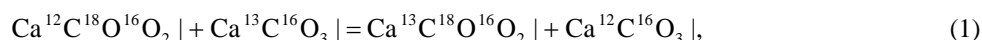¹³C-¹⁸O clumping effects [1]-[3] in carbonates play significant roles in reconstructing the temperatures in geological research [4]-[9]. The majority of data points of ¹³C-¹⁸O signals of CO_2 extracted from carbonate minerals is explained by the equilibrium isotope reactions on the growth surfaces of crystals during their formation [10]. However, there still exist some measured data points which deviate from our predicted Δ_{47} polynomials of pure

aragonite and calcite [10]. And one hypothesis for solving this problem was that during the crystallization of minerals, the carbonates captured the metal cations (M^{2+}) from solutions and these cations influenced the ^{13}C-^{18}O isotope signals in turn.

To prove our hypothesis, this paper studied the effects of Mg^{2+}, Fe^{2+} and Zn^{2+} cations on the ^{13}C-^{18}O bonds in aragonite, calcite and dolomite. We gave the novel relationships of Δ_{47} with respect to temperatures for different M^{2+}-carbonate systems, and gave suggestions on the utilization of present results to understand the formation temperatures of carbonates in different geological systems. Finally, the theoretical value of the influence of phosphoric acid on Δ_{47} of CO_2 degassed from different carbonates was discussed.

2. Methodology

For ^{13}C-^{18}O clumped effect on the surfaces of, for example, calcite and aragonite [10], we have isotope reaction

$$Ca\,^{12}C\,^{18}O\,^{16}O_2\,| + Ca\,^{13}C\,^{16}O_3\,| = Ca\,^{13}C\,^{18}O\,^{16}O_2\,| + Ca\,^{12}C\,^{16}O_3\,|, \tag{1}$$

where "|" stands for the surface of minerals. The equilibrium constant K3866| (illustrating the doubly substituted isotopologues $^{13}C^{18}O^{16}O_2^{2-}$ in the reaction) for prior reaction is

$$K3866| = \frac{\left[Ca\,^{13}C\,^{18}O\,^{16}O_2\,|\right]\left[Ca\,^{12}C\,^{16}O_3\,|\right]}{\left[Ca\,^{12}C\,^{18}O\,^{16}O_2\,|\right]\left[Ca\,^{13}C\,^{16}O_3\,|\right]}, \tag{2}$$

where the brackets indicate the concentrations of the isotopologues [4] [11]. And ^{13}C-^{18}O clumped bonds in this reaction are kept in the body of calcite and aragonite [10], according to different crystal growth model (e.g. "growth entrapment model" [12]-[14] and "surface kinetic model" [15]).

The interfacial clusters of carbonate groups on calcite (0001) surface, aragonite (001) surface and dolomite (0001) surfaces (**Figure 1**) were built with *ab initio* technique in Yuan *et al.* (2014). All structures had 3 layers of atoms extracted from periodical crystals, which represent the surface of crystal, and six water molecules, which represent the solution. The atoms in the crystals were terminated with charge points (calcite, 0.333; aragonite, 0.222; dolomite, 0.333) [16] at 1 Å along the broken Ca (or Mg)-O bond [17]. Before optimized, the Ca, Mg, C and O positions were the same as those in corresponding lattices (**Table 1**). And the first metal atoms in
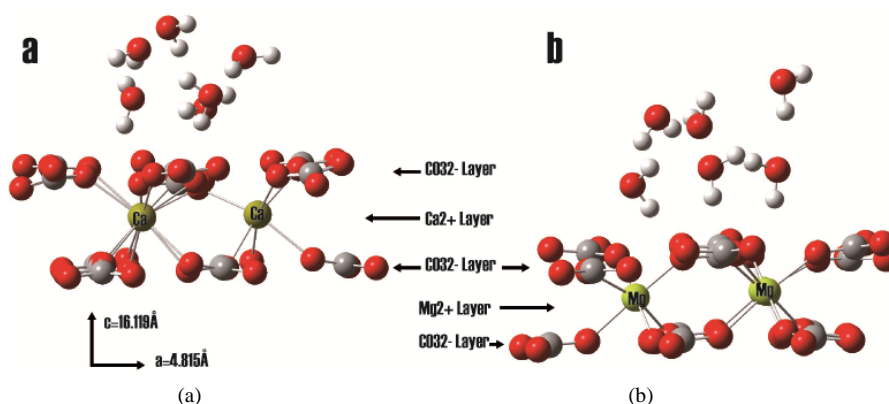

Figure 1. Optimized clusters of a) Ca^{2+}-layer and b) Mg^{2+}-layer dolomite (0001) surface at HF/6-31G*. Because dolomite has an alternating structural arrangement (shown in middle) of calcium and magnesium ions, their influence on carbonate group is considered by using simplified clusters of Ca^{2+}-layer and Mg^{2+}-layer dolomite respectively.

Table 1. Crystal structures of pure carbonate minerals used for building clusters.

Minerals	Space group	a(Å)	b(Å)	c(Å)	Ref.
Aragonite [CaCO₃]	*Pmcn*	4.96	7.97	5.74	[23]
Calcite [CaCO₃]	$R\bar{3}c$	4.99		17.06	[24]
Dolomite [CaMg(CO₃)₂]	$R\bar{3}$	4.82		16.12	[25]

each cluster were substituted by Fe^{2+}, Mg^{2+} or Zn^{2+} cations to study their influence on Δ_{47}, RPFR($^{13/12}$C), RPFR($^{14/12}$C) and RPFR($^{18/16}$O); see Supplementary File for the orientations of atoms in different clusters. Please reference Yuan *et al.* (2014) for the structures of aragonite (001) and calcite (0001) surfaces.

All these clusters were optimized in the Gaussian09 code [16]. The theoretical method was HF [18], and the basis set was 6 - 31G* [19] [20], which are suitable for C, Ca, Fe, Mg, O and Zn elements. The theoretical equilibrium constant of reaction (1) was calculated by

$$K3866| = \frac{RPFR\left(Ca^{13/12}C^{18}O^{16}O_2|\right)}{RPFR\left(Ca^{13/12}C^{16}O_3|\right)}, \tag{3}$$

of which RPFR (short for reduced partition function ratio) [21] [22] is given by

$$RPFR\left[X^{h/l}E_K\right] = \prod_i^{3N-6} \frac{u_i\left(XE_K^h\right)}{u_i\left(XE_K^l\right)} \frac{\exp\left[-u_i\left(XE_K^h\right)/2\right]}{\exp\left[-u_i\left(XE_K^l\right)/2\right]} \frac{\left\{1-\exp\left[-u_i\left(XE_K^l\right)\right]\right\}}{\left\{1-\exp\left[-u_i\left(XE_K^h\right)\right]\right\}}, \tag{4}$$

where XE_K stands for the molecule, h and l represent heavy (^{13}C, ^{18}O) and light (^{12}C, ^{16}O) isotopes of element E, $u = hv_i/kT$, h is the Planck constant, v_i is the ith frequency of our clusters given by Gaussian09 [16], k is the Boltzmann constant, and T is the temperature from 260 to 1500 K [4] [5] [10]. When calculating RPFRs, scaling factor SF = 1.0613 for HF/6-31G* level was used, which is suggested by Yuan *et al.* (2014) for research on isotope effect on interfaces of carbonates.

Specifically, as shown in **Table 2**, one aragonite and four dolomite clusters had few imaginary vibrational frequencies; and in such case we used the reduced partition function ratio in the frequency complex plane (RPFR$_C$) to predict the isotope fractionation factor in these clusters [26].

Present theoretical Δ_{47} and Δ_{63} were calculated by

$$\Delta_{47} = \Delta_{63} \cong 1000 \times \left(K3866|-1\right), \tag{5}$$

which is within accuracy of 94% [4]-[7] [10]. All Δ_{63} values of the carbonates were given by averaging those of three different oxygen sites (O$_1$, O$_2$ and O$_3$) [10]. See reasons for $\Delta_{47} = \Delta_{63}$ in next section.

3. Results and Discussion

The calculated structures of dolomite are shown in **Figure 1**. The polynomials of Δ_{47} and RPFRs ($^{13/12}$C, $^{14/12}$C [27] and $^{18/16}$O) in pure and metal-cations-influenced aragonite, calcite and dolomite, and their corresponding values at 25°C are listed in **Table 3** and **Table 4**, respectively; plots of these polynomials are in **Figure 2**. The comparison of Δ_{47} of dolomite between different theoretical works is illustrated in **Figure 3**.

3.1. Effect of Metal Cations on Different Isotope Systems

The metal cations in precipitated carbonates cause the decrease of Δ_{47} values (at 25°C) from pure carbonates. For impurity aragonite, Δ_{47} values are 0.036 (Mg^{2+}), 0.030 (Fe^{2+}) and 0.042 (Zn^{2+}) lower than that of pure crystal. For impurity calcite, Δ_{47} values are 0.032 (Mg^{2+}), 0.035 (Fe^{2+}) and 0.022 (Zn^{2+}) lower than that of pure crystal. For

Table 2. Summary of imaginary frequencies of dolomite clusters at HF/6-31G* level (Yuan, 2014). n is the number of imaginary frequency. The minimal and maximal frequencies are shown.

Cluster	n	Minimal*	Maximal*
Fe^{2+}-Aragonite	1	−26.7666	−26.7666
Pure-Dolomite (Ca^{2+}-layer)	1	−177.475	−177.475
Fe^{2+}-Dolomite (Ca^{2+}-layer)	1	−88.0780	−88.0780
Zn^{2+}-Dolomite (Ca^{2+}-layer)	2	−83.2690	−27.5030
Pure-Dolomite (Mg^{2+}-layer)	3	−134.690	−50.3736

*The frequencies correspond to molecules with $M^{2+}\,^{12}C^{16}O^{16}O^{16}O^{2-}$.
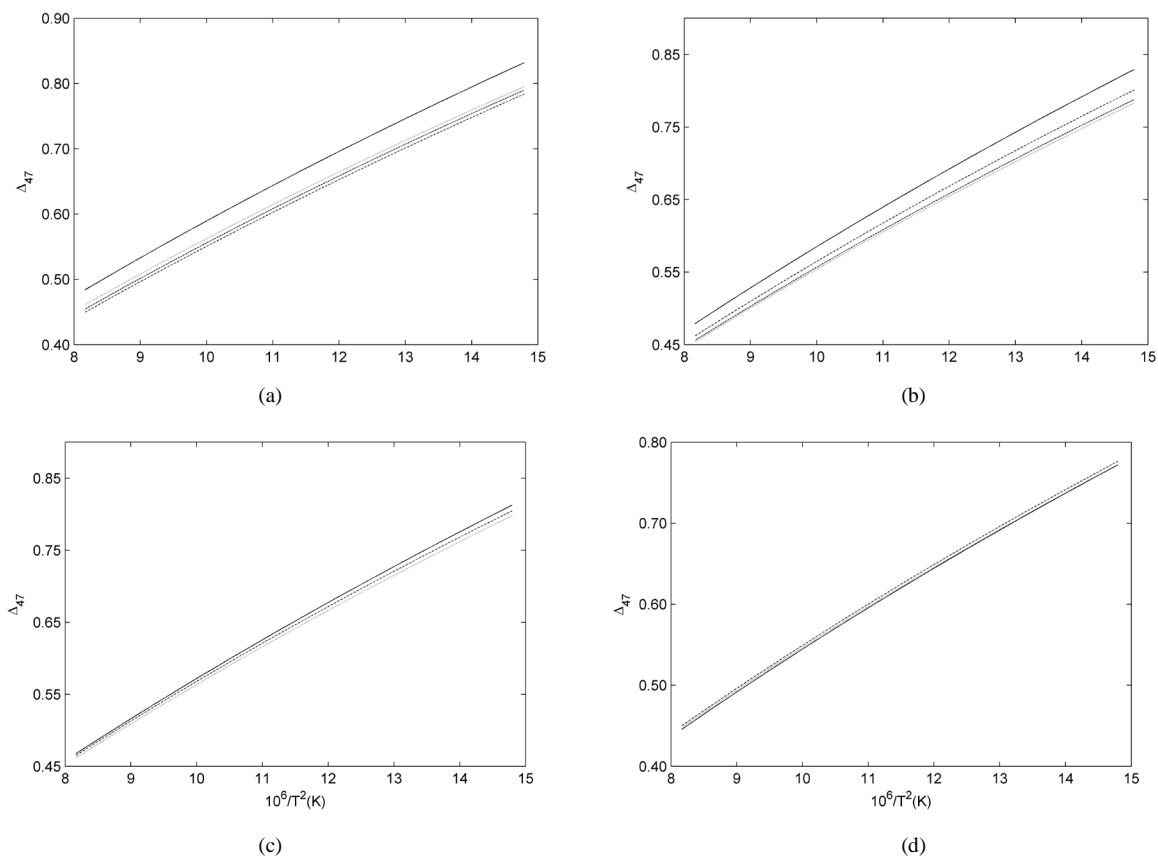
Figure 2. Influence of Mg^{2+} (dashed), Fe^{2+} (dotted) and Zn^{2+} (dash-dotted) ions on Δ_{47} values in (a) aragonite; (b) calcite and (c) Ca^{2+}-layer dolomite and (d) Mg^{2+}-layer dolomite. For comparison, Δ_{47} values in pure minerals are shown in solid lines. Temperatures range from 260 to 350 K.
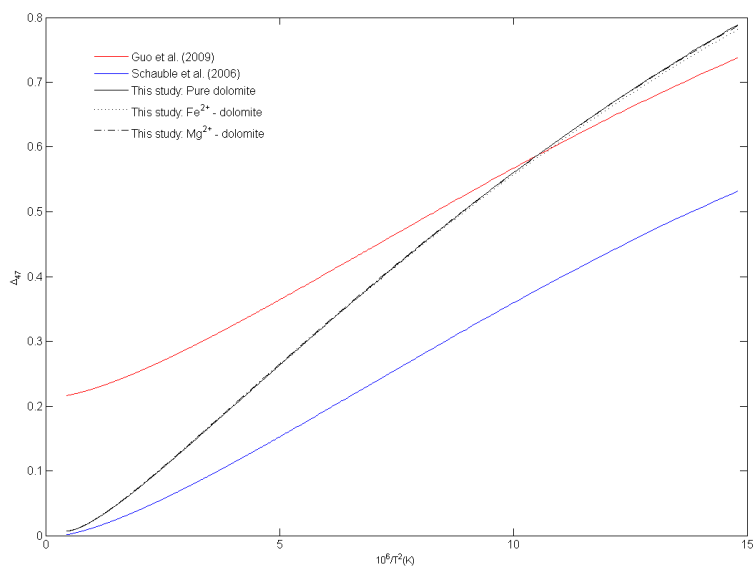

Figure 3. Comparison of Δ_{47} values of dolomite between different theoretical works: Schauble *et al.* (2006), blue solid; Guo *et al.* (2009), red solid; This work: pure dolomite, black solid; Fe^{2+}-dolomite, black dotted; Zn^{2+}-dolomite, black dash-dotted. Temperatures range from 260 to 1500 K.

Table 3. Parameters of fitted polynomials of Δ_{47}, RPFR($^{13/12}$C), RPFR($^{14/12}$C) RPFR($^{18/16}$O) for aragonite, calcite and dolomite.

Minerals	Metal Cation	Items*	A	B	C	D	E	Error**
Aragonite	Mg^{2+}	Δ_{47}	−1.04823E+09	−6.34189E+06	1.28767E+05	−1.50928E+02	5.22169E−02	0.025588
		RPFR($^{13/12}$C)	6.59513E+08	−7.98499E+06	4.43257E+04	−2.95208	1.00028	0.000971
		RPFR($^{14/12}$C)	1.09916E+09	−1.22585E+07	8.07321E+04	−5.72922	1.00086	0.001297
		RPFR($^{18/16}$O)	2.05776E+08	−2.92886E+06	1.99938E+04	−2.04600	1.00046	0.000129
	Fe^{2+}	Δ_{47}	−7.91119E+08	−9.18801E+06	1.38333E+05	−1.59586E+02	5.48161E−02	0.025974
		RPFR($^{13/12}$C)	6.72557E+08	−8.09753E+06	4.47485E+04	−2.71504	1.00019	0.001034
		RPFR($^{14/12}$C)	1.12550E+09	−1.24567E+07	8.16035E+04	−5.39957	1.00072	0.001397
		RPFR($^{18/16}$O)	2.15376E+08	−3.02739E+06	2.05065E+04	−2.01891	1.00044	0.000151
	Zn^{2+}	Δ_{47}	−1.16339E+09	−5.10126E+06	1.24375E+05	−1.47117E+02	5.10630E−02	0.025410
		RPFR($^{13/12}$C)	6.50322E+08	−7.90122E+06	4.40135E+04	−3.09137	1.00034	0.000931
		RPFR($^{14/12}$C)	1.08164E+09	−1.21147E+07	8.00991E+04	−5.91487	1.00094	0.001235
		RPFR($^{18/16}$O)	2.00842E+08	−2.86872E+06	1.97261E+04	−2.03180	1.00046	0.000123
Calcite	Mg^{2+}	Δ_{47}	−7.76602E+08	−9.02892E+06	1.36577E+05	−1.57698E+02	5.42061E−02	0.025746
		RPFR($^{13/12}$C)	6.69044E+08	−8.06860E+06	4.46748E+04	−2.77108	1.00021	0.001020
		RPFR($^{14/12}$C)	1.11826E+09	−1.23973E+07	8.14323E+04	−5.46645	1.00075	0.001376
		RPFR($^{18/16}$O)	2.15909E+08	−3.03256E+06	2.03398E+04	−2.01788	1.00044	0.000154
	Fe^{2+}	Δ_{47}	−7.56772E+08	−9.26436E+06	1.36975E+05	−1.58160E+02	5.43133E−02	0.025704
		RPFR($^{13/12}$C)	6.68928E+08	−8.06351E+06	4.46644E+04	−2.74379	1.00020	0.001023
		RPFR($^{14/12}$C)	1.11897E+09	−1.23905E+07	8.14193E+04	−5.42064	1.00073	0.001382
		RPFR($^{18/16}$O)	2.16575E+08	−3.04422E+06	2.05701E+04	−2.03322	1.00044	0.000152
	Zn^{2+}	Δ_{47}	−9.35476E+08	−7.74939E+06	1.34750E+05	−1.57121E+02	5.41471E−02	0.026023
		RPFR($^{13/12}$C)	6.71475E+08	−8.09220E+06	4.46908E+04	−2.79787	1.00022	0.001022
		RPFR($^{14/12}$C)	1.12223E+09	−1.24513E+07	8.14887E+04	−5.54266	1.00077	0.001374
		RPFR($^{18/16}$O)	2.08364E+08	−2.95897E+06	2.01945E+04	−2.01893	1.00044	0.000137
Dolomite: Ca^{2+} Layer	Pure	Δ_{47}	−1.00183E+09	−7.29348E+06	1.35024E+05	−1.58331E+02	5.46361E−02	0.026382
		RPFR($^{13/12}$C)	6.80247E+08	−8.18193E+06	4.49968E+04	−2.84015	1.00022	0.001041
		RPFR($^{14/12}$C)	1.13701E+09	−1.26061E+07	8.20891E+04	−5.67425	1.00080	0.001397
		RPFR($^{18/16}$O)	2.05630E+08	−2.92663E+06	2.00567E+04	−2.01773	1.00045	0.000131
	Fe^{2+}	Δ_{47}	−8.63868E+08	−8.45111E+06	1.36372E+05	−1.57956E+02	5.43307E−02	0.025868
		RPFR($^{13/12}$C)	6.75687E+08	−8.12957E+06	4.48533E+04	−2.72920	1.00019	0.001040
		RPFR($^{14/12}$C)	1.13075E+09	−1.25128E+07	8.18125E+04	−5.44681	1.00073	0.001403
		RPFR($^{18/16}$O)	2.08778E+08	−2.95887E+06	2.03216E+04	−2.00660	1.00044	0.000138
	Zn^{2+}	Δ_{47}	−8.51760E+08	−8.61298E+06	1.37582E+05	−1.59285E+02	5.47580E−02	0.025958

Continued

		RPFR($^{13/12}$C)	6.78268E+08	−8.15043E+06	4.48767E+04	−2.67332	1.00017	0.001056
		RPFR($^{14/12}$C)	1.13581E+09	−1.25603E+07	8.18894E+04	−5.37669	1.00070	0.001429
		RPFR($^{18/16}$O)	2.08127E+08	−2.95288E+06	2.02734E+04	−1.98940	1.00043	0.000138
Dolomite: Mg^{2+} Layer	Pure	Δ_{47}	−1.03324E+09	−6.52344E+06	1.27815E+05	−1.50058E+02	5.19586E−02	0.025629
		RPFR($^{13/12}$C)	6.64267E+08	−8.04237E+06	4.46862E+04	−3.09732	1.00033	0.000961
		RPFR($^{14/12}$C)	1.10669E+09	−1.23236E+07	8.13566E+04	−5.98283	1.00094	0.001269
		RPFR($^{18/16}$O)	2.07005E+08	−2.93561E+06	2.02598E+04	−2.06050	1.00046	0.000131
	Fe^{2+}	Δ_{47}	−8.86768E+08	−8.16381E+06	1.33099E+05	−1.54806E+02	5.33692E−02	0.025810
		RPFR($^{13/12}$C)	6.73343E+08	−8.12003E+06	4.49981E+04	−2.91796	1.00026	0.001005
		RPFR($^{14/12}$C)	1.12531E+09	−1.24573E+07	8.19949E+04	−5.72788	1.00084	0.001338
		RPFR($^{18/16}$O)	2.12319E+08	−2.99620E+06	2.07317E+04	−2.05617	1.00045	0.000140
	Zn^{2+}	Δ_{47}	−8.85943E+08	−8.14695E+06	1.33368E+05	−1.55041E+02	5.34493E−02	0.025816
		RPFR($^{13/12}$C)	6.73842E+08	−8.12314E+06	4.49739E+04	−2.89586	1.00025	0.001011
		RPFR($^{14/12}$C)	1.12627E+09	−1.24698E+07	8.19650E+04	−5.69849	1.00083	0.001348
		RPFR($^{18/16}$O)	2.12267E+08	−2.99350E+06	2.06000E+04	−2.04615	1.00045	0.000142
Dolomite: Mean***	Pure	Δ_{47}	−1.01754E+09	−6.90846E+06	1.31419E+05	−1.54194E+02	5.32973E−02	0.026006
		RPFR($^{13/12}$C)	6.72257E+08	−8.11215E+06	4.48415E+04	−2.96874	1.00028	0.001001
		RPFR($^{14/12}$C)	1.12185E+09	−1.24649E+07	8.17229E+04	−5.82854	1.00087	0.001333
		RPFR($^{18/16}$O)	2.06317E+08	−2.93112E+06	2.01583E+04	−2.03912	1.00045	0.000131
	Fe^{2+}	Δ_{47}	−8.75318E+08	−8.30746E+06	1.34735E+05	−1.56381E+02	5.38499E−02	0.025839
		RPFR($^{13/12}$C)	6.74515E+08	−8.12480E+06	4.49257E+04	−2.82358	1.00023	0.001023
		RPFR($^{14/12}$C)	1.12803E+09	−1.24851E+07	8.19037E+04	−5.58734	1.00078	0.001370
		RPFR($^{18/16}$O)	2.10549E+08	−2.97754E+06	2.05266E+04	−2.03139	1.00045	0.000139
	Zn^{2+}	Δ_{47}	−8.68852E+08	−8.37996E+06	1.35475E+05	−1.57163E+02	5.41036E−02	0.025887
		RPFR($^{13/12}$C)	6.76055E+08	−8.13678E+06	4.49253E+04	−2.78459	1.00021	0.001033
		RPFR($^{14/12}$C)	1.13104E+09	−1.25151E+07	8.19272E+04	−5.53759	1.00076	0.001389
		RPFR($^{18/16}$O)	2.10197E+08	−2.97319E+06	2.04367E+04	−2.01777	1.00044	0.000140

*The form of each fit is $f(T) = A/T^4 + B/T^3 + C/T^2 + D/T + E$. **The errors stand for the values within which these polynomials reproduce the equilibrium constants from 260 to 1500 K. ***The polynomials of different dolomites are given by averaging those of Ca^{2+}-layer dolomite and Mg^{2+}-layer dolomite.

impurity dolomite, Δ_{47} value is 0.004 (Fe^{2+}) lower than that of pure crystal.

The decrease of Δ_{47} caused by metal cations would increase the formation temperatures of minerals, when geochemists reconstruct temperatures with the fitted polynomials, e.g. $\Delta_{47} = 0.0592 \times 10^6 / T^2 - 0.02$ in Ghosh *et al.* (2006) (and calibrated ones in later works [9] [28]), from experimental data. For instance, if we got $\Delta_{47} = 0.615$ in a zinc-enriched (~33% in content) aragonite, then we get temperature $T = 32.2°C$ from the polynomials in Ghosh *et al.* (2006). However, the exact temperature is 25°C (**Table 4**), 7.2°C (= 32.2°C - 25°C) lower than the predicted value. Thus, aiming to get formation temperatures with high accuracy, we suggest that a researcher would better measure the main metal impurities in carbonates before choosing a reasonable ^{13}C-^{18}O clumped thermometer (as shown in **Table 3**).

Table 4. Values of Δ_{47}, RPFR($^{13/12}$C), RPFR($^{14/12}$C) and RPFR($^{18/16}$O) for carbonates at 25°C.

Minerals	Metal Ion	Δ_{47}	RPFR($^{13/12}$C)	RPFR($^{14/12}$C)	RPFR($^{18/16}$O)
Aragonite	Pure	0.657	1.2785	1.5832	1.1394
	Mg^{2+}	0.621	1.2713	1.5665	1.1341
	Fe^{2+}	0.627	1.2742	1.5732	1.1374
	Zn^{2+}	0.615	1.2694	1.5621	1.1327
Calcite	Pure	0.653	1.2761	1.5777	1.1355
	Mg^{2+}	0.621	1.2738	1.5724	1.1354
	Fe^{2+}	0.618	1.2739	1.5727	1.1376
	Zn^{2+}	0.631	1.2733	1.5712	1.1356
Dolomite: Ca^{2+} Layer	Pure	0.639	1.2743	1.5736	1.1349
	Fe^{2+}	0.629	1.2745	1.5739	1.1371
	Zn^{2+}	0.634	1.2744	1.5738	1.1368
Dolomite: Mg^{2+} Layer	Pure	0.608	1.2733	1.5713	1.1369
	Fe^{2+}	0.610	1.2756	1.5765	1.1406
	Zn^{2+}	0.613	1.2753	1.5759	1.1393
Dolomite: Mean	Pure	0.623	1.2738	1.5724	1.1359
	Fe^{2+}	0.619	1.2750	1.5752	1.1389
	Zn^{2+}	0.623	1.2749	1.5749	1.1380

These metal cations also significantly influence on the fractionations of $^{13/12}$C, $^{14/12}$C and $^{18/16}$O isotope systems. The isotope fractionation factor (at 25°C) between the impurity mineral and corresponding pure one is defined as $\Delta_{\text{metal ion-pure}}$ (in *per mil* or ‰) = 1000 * ln(RPFR$_{\text{(Metal ion)}}$/RPFR$_{\text{pure}}$). For aragonite, $\Delta(^{13/12}$C)s are −5.7 (Mg^{2+}), −3.4 (Fe^{2+}) and −7.2 (Zn^{2+}); $\Delta(^{14/12}$C)s are −10.6 (Mg^{2+}), −6.4 (Fe^{2+}) and −13.4 (Zn^{2+}); and $\Delta(^{18/16}$O)s are −4.7 (Mg^{2+}), −1.8 (Fe^{2+}) and −5.9 (Zn^{2+}). For calcite, $\Delta(^{13/12}$C)s are −1.8 (Mg^{2+}), −1.7 (Fe^{2+}) and −2.2 (Zn^{2+}); $\Delta(^{14/12}$C)s are −3.4 (Mg^{2+}), −3.2 (Fe^{2+}) and −4.1 (Zn^{2+}); $\Delta(^{18/16}$O)s are −0.1 (Mg^{2+}), −1.8 (Fe^{2+}) and 0.1 (Zn^{2+}). For dolomite, $\Delta(^{13/12}$C)s are −0.9 (Fe^{2+}) and −0.8 (Zn^{2+}); $\Delta(^{14/12}$C)s are 1.8 (Fe^{2+}) and 1.6 (Zn^{2+}); and $\Delta(^{18/16}$O)s are 2.6 (Fe^{2+}) and 1.8 (Zn^{2+}). Obviously, most of the magnitudes of these three metal ions on the $^{13/12}$C, $^{14/12}$C and $^{18/16}$O fractionations are at the level of 1 *per mil*, and few 10 *per mil*s. Such magnitudes might be observed in laboratories.

Our above finding is different from that given by Schauble *et al.* (2006) (**Figure 3**), which concluded that M^{2+}-cations have little influence on isotopic fractionations between carbonate minerals. The reasons behind the difference were: 1) the ^{13}C-^{18}O clumped effect on growing surfaces of minerals was studied here, while this effect in the inner body of crystals were predicted with lattice dynamics in their paper; and 2) the force constants for, for example, Fe^{2+}-calcite differ from those for Mg^{2+}-calcite in this work, while these values for ^{40}BaCO$_3$ and ^{40}MgCO$_3$ are identical in their lattice-dynamical models.

3.2. Theoretical Value y of Influence of Phosphoric Acid on ^{13}C-^{18}O Bonds in Carbonates

In ^{13}C-^{18}O clumped isotope research, anyone cannot avoid the influence of phosphoric acid in experiments [4]-[6] [29] [30]; and now we give the theoretical value y_{theory} of its influence on the Δ_{47} values of CO$_2$ extracted from carbonates, by studying the equilibrium reaction $2H^+ + CO_3^{2-} = H_2O + CO_2 \uparrow$ in this process (**Figure 4**). Let

$N_{CO_3^{2-}}^{^{13}C\text{-}^{18}O}$, $N_{CO_3^{2-}}^{^{12}C\text{-}^{18}O}$, $N_{CO_3^{2-}}^{^{13}C\text{-}^{16}O}$ and $N_{CO_3^{2-}}^{^{12}C\text{-}^{16}O}$ respectively denote the number of $^{13}C\text{-}^{18}O$, $^{12}C\text{-}^{18}O$, $^{13}C\text{-}^{16}O$ and $^{12}C\text{-}^{16}O$ bonds in carbonate minerals. Then from Equation (5), we have

$$\Delta_{63} = 1000 \times \left(\frac{\dfrac{N_{CO_3^{2-}}^{^{13}C\text{-}^{18}O}}{N_{CO_3^{2-}}^{^{12}C\text{-}^{18}O}}}{\dfrac{N_{CO_3^{2-}}^{^{13}C\text{-}^{16}O}}{N_{CO_3^{2-}}^{^{12}C\text{-}^{16}O}}} - 1 \right) \tag{6}$$

Let $N_{CO_2}^{^{13}C\text{-}^{18}O}$, $N_{CO_2}^{^{12}C\text{-}^{18}O}$, $N_{CO_2}^{^{13}C\text{-}^{16}O}$ and $N_{CO_2}^{^{12}C\text{-}^{16}O}$ respectively denote the number of $^{13}C\text{-}^{18}O$, $^{12}C\text{-}^{18}O$, $^{13}C\text{-}^{16}O$ and $^{12}C\text{-}^{16}O$ bonds in CO_2 degassed from carbonate minerals with phosphoric acid. Then similar to prior equation [1] [31], the corresponding Δ_{47} is given by

$$\Delta_{47} = 1000 \times \left(\frac{\dfrac{N_{CO_2}^{^{13}C\text{-}^{18}O}}{N_{CO_2}^{^{12}C\text{-}^{18}O}}}{\dfrac{N_{CO_2}^{^{13}C\text{-}^{16}O}}{N_{CO_2}^{^{12}C\text{-}^{16}O}}} - 1 \right) \tag{7}$$

The relationship between Δ_{47} and Δ_{63} are given according to the probability theory [32]. Firstly, the probability of the occupation of one $^{13}C\text{-}^{18}O$ bond on each of three different carbon-oxygen (C-O1, C-O2 or C-O3) bonds in $^xC^xO^{16}O_2^{2-}$ is 1/3 (**Figure 4**); secondly, the probability of one oxygen site (O1, O2, or O3) connecting with two H+s is also 1/3. After the water molecule, for example, H2O1 formed, one-third of $^{13}C\text{-}^{18}O$ bonds are removed from $^xC^xO^{16}O_2^{2-}$, leaving other two-thirds of such bonds in $^xC^xO^{16}O$; that is, the number of $^{13}C\text{-}^{18}O$ bonds decrease one-third from $^xC^xO^{16}O_2^{2-}$ to $^xC^xO^{16}O$ during the reaction. Similarly to $^{13}C\text{-}^{18}O$ bond, the same probability 1/3 is true for $^{12}C\text{-}^{18}O$, $^{13}C\text{-}^{16}O$ and $^{12}C\text{-}^{16}O$ bonds during the reaction. Finally, we theoretically have

$$\Delta_{47} = 1000 \times \left(\frac{\dfrac{N_{CO_2}^{^{13}C\text{-}^{18}O}}{N_{CO_2}^{^{12}C\text{-}^{18}O}}}{\dfrac{N_{CO_2}^{^{13}C\text{-}^{16}O}}{N_{CO_2}^{^{12}C\text{-}^{16}O}}} - 1 \right) = 1000 \times \left(\frac{\dfrac{N_{CO_3^{2-}}^{^{13}C\text{-}^{18}O} - \frac{1}{3}N_{CO_3^{2-}}^{^{13}C\text{-}^{18}O}}{N_{CO_3^{2-}}^{^{12}C\text{-}^{18}O} - \frac{1}{3}N_{CO_3^{2-}}^{^{12}C\text{-}^{18}O}}}{\dfrac{N_{CO_3^{2-}}^{^{13}C\text{-}^{16}O} - \frac{1}{3}N_{CO_3^{2-}}^{^{13}C\text{-}^{16}O}}{N_{CO_3^{2-}}^{^{12C-16O}} - \frac{1}{3}N_{CO_3^{2-}}^{^{12}C\text{-}^{16}O}}} - 1 \right),$$

$$= 1000 \times \left(\frac{\dfrac{\frac{2}{3}N_{CO_3^{2-}}^{^{13}C\text{-}^{18}O}}{\frac{2}{3}N_{CO_3^{2-}}^{^{12}C\text{-}^{18}O}}}{\dfrac{\frac{2}{3}N_{CO_3^{2-}}^{^{13}C\text{-}^{16}O}}{\frac{2}{3}N_{CO_3^{2-}}^{^{12}C\text{-}^{16}O}}} - 1 \right) = 1000 \times \left(\frac{\dfrac{N_{CO_3^{2-}}^{^{13}C\text{-}^{18}O}}{N_{CO_3^{2-}}^{^{12}C\text{-}^{18}O}}}{\dfrac{N_{CO_3^{2-}}^{^{13}C\text{-}^{16}O}}{N_{CO_3^{2-}}^{^{12}C\text{-}^{16}O}}} - 1 \right) = \Delta_{63}, \tag{8}$$

which shows that the Δ_{63} value kept in carbonate is identical to the Δ_{47} value in CO_2 degassed from the carbonate with phosphoric acid.

Then the theoretical value $y_{theory} = \Delta_{47} - \Delta_{63}$ [7] [10] $= 0$ is given here, and is suggested to be used in theoretical predictions, such as first-principle calculations in present paper.

The relationship between y_{theory} and $y_{exp.}$ is addressed as following. For experimental geochemists in the laboratories, the value of $y_{exp.}$ obeys the rule of counting statistics, and is proportional to $1/\sqrt{N}$ where N is the number of times they analyzed one sample (See [6] [33] for more information). Obviously, if N is large enough,
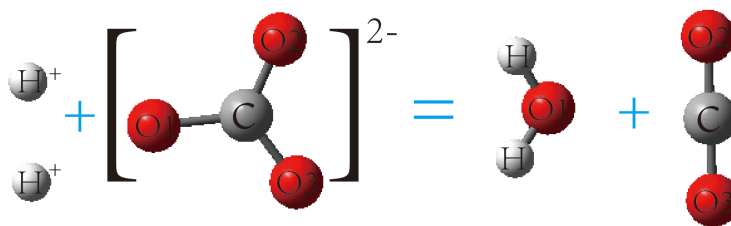
Figure 4. Illustration of equilibrium reaction $2H^+ + CO_3^{2-} = H_2O + CO_2 \uparrow$ during the process of extracting CO_2 from carbonates with phosphoric acid (H_3PO_4). The hydrogen ion H^+ is ionized from phosphoric acid; the carbonate group CO_3^{2-} comes from carbonate minerals. Three different oxygen sites of the carbonate group are labeled as O1, O2, and O3. Other chemical reactions (e.g. $H_3PO_4 = 3H^+ + PO_4^{3-}$ and $3Ca^{2+} + 2PO_4^{3-} = Ca_3(PO_4)_2$ etc.) in this process (McCrea, 1950; Swart *et al.*, 1991) are omitted since they do not significantly contribute to ^{13}C-^{18}O clumped isotope research.

then

$$\lim_{N \to \infty} y_{exp} \propto \lim_{N \to \infty} \frac{1}{\sqrt{N}} = 0 = y_{theory}. \qquad 9)$$

Present $y_{theory} = 0$ differs from that (e.g. 0.232‰ ± 0.015‰ for calcite) given by Guo *et al.* (2009) (**Figure 3**). The main difference between their and present works came from the following fact: when studying the phosphoric acid digestion, they investigated the possible kinetic isotope effect caused by the transition state of dissociation of H_2CO_3 intermediate in non-equilibrium reaction $H_2CO_3 \to (2H^+ \cdot O^{2-}) \cdot CO_2$ (the transition state) $\to H_2O + CO_2 \uparrow$, while present paper focused on the equilibrium isotope effect caused by deoxidizing the carbonate group (CO_3^{2-}) in equilibrium reaction $2H^+ + CO_3^{2-} = H_2O + CO_2 \uparrow$. Here, we suggest that if the duration of the phosphoric acid digestion is long enough (e.g. 16 h in Ghosh *et al.* (2006) and 24 h in Guo *et al.* (2009)), then the digestion reaction was an equilibrium one [34].

4. Conclusions

The influence of Mg^{2+}, Fe^{2+} and Zn^{2+} cations on ^{13}C-^{18}O bonds in aragonite, calcite and dolomite was studied using *ab initio* quantum calculations. And we can draw the following conclusions:

1) The metal ions significantly influenced the ^{13}C-^{18}O clumping bonds (as well as $^{13/12}C$, $^{14/12}C$ and $^{18/16}O$ isotope information) in the process of precipitation of and finally the body of aragonite, calcite and dolomite. Due to this influence, we suggested that when using the polynomials of ^{13}C-^{18}O clumping bonds in these minerals to predict temperatures, it would be better for a researcher to firstly determine the chemical composition of metal cations in carbonates, and secondly choose a reasonable thermometer according to the main metal impurities in the minerals.

2) Based on the probability theory, the value of the influence of phosphoric acid on ^{13}C-^{18}O clumping bonds during the extracting process of CO_2 from carbonates was zero for theoretical research, e.g. first-principle calculations in this study. And the magnitude of this value in the experiments is proportional to the counting statistics.

Acknowledgements

References

[1] Wang, Z.G., Schauble, E.A. and Eiler, J.M. (2004) Equilibrium Thermodynamics of Multiply Substituted Isotopologues of Molecular Gases. *Geochimica et Cosmochimica Acta*, **68**, 4779-4797.
http://dx.doi.org/10.1016/j.gca.2004.05.039

[2] Eiler, J.M. (2007) "Clumped-Isotope" Geochemistry—The Study of Naturally-Occurring, Multiply-Substituted Isotopologues. *Earth and Planetary Science Letters*, **262**, 309-327. http://dx.doi.org/10.1016/j.epsl.2007.08.020

[3] Eiler, J.M. and Schauble, E. (2004) $^{18}O^{13}C^{16}O$ in Earth's Atmosphere. *Geochimica et Cosmochimica Acta*, **68**, 4767-4777. http://dx.doi.org/10.1016/j.gca.2004.05.035

[4] Schauble, E.A., Ghosh, P. and Eiler, J.M. (2006) Preferential Formation of ^{13}C-^{18}O Bonds in Carbonate Minerals, Estimated Using First-Principles Lattice Dynamics. *Geochimica et Cosmochimica Acta*, **70**, 2510-2529. http://dx.doi.org/10.1016/j.gca.2006.02.011

[5] Guo, W.F., Mosenfelder, J.L., Goddard, W.A. and Eiler, J.M. (2009) Isotopic Fractionations Associated with Phosphoric Acid Digestion of Carbonate Minerals: Insights from First-Principles Theoretical Modeling and Clumped Isotope Measurements. *Geochimica et Cosmochimica Acta*, **73**, 7203-7225. http://dx.doi.org/10.1016/j.gca.2009.05.071

[6] Ghosh, P., Adkins, J., Affek, H., Balta, B., Guo, W.F., Schauble, E.A., *et al.* (2006) ^{13}C-^{18}O Bonds in Carbonate Minerals: A New Kind of Paleothermometer. *Geochimica et Cosmochimica Acta*, **70**, 1439-1456. http://dx.doi.org/10.1016/j.gca.2005.11.014

[7] Hill, P.S., Tripati, A.K. and Schauble, E.A. (2014) Theoretical Constraints on the Effects of pH, Salinity, and Temperature on Clumped Isotope Signatures of Dissolved Inorganic Carbon Species and Precipitating Carbonate Minerals. *Geochimica et Cosmochimica Acta*, **125**, 610-652. http://dx.doi.org/10.1016/j.gca.2013.06.018

[8] Dennis, K.J. and Schrag, D.P. (2010) Clumped Isotope Thermometry of Carbonatites as an Indicator of Diagenetic Alteration. *Geochimica et Cosmochimica Acta*, **74**, 4110-4122. http://dx.doi.org/10.1016/j.gca.2013.06.018

[9] Ghosh, P., Eiler, J., Campana, S.E. and Feeney, R.F. (2007) Calibration of the Carbonate "Clumped Isotope" Paleothermometer for Otoliths. *Geochimica et Cosmochimica Acta*, **71**, 2736-2744. http://dx.doi.org/10.1016/j.gca.2007.03.015

[10] Yuan, J., Zhang, Z. and Zhang, Y. (2014) ^{13}C-^{18}O Bonds in Precipitated Calcite and Aragonite: An *ab Initio* Study. *Open Journal of Geology*, **4**, 436-480. http://dx.doi.org/10.4236/ojg.2014.49034

[11] Schauble, E.A. and Eiler, J.M. (2004) Theoretical Estimates of Equilibrium ^{13}C-^{18}O Clumping in Carbonates and Organic Acids. *Eos*, *Transactions American Geophysical Union*, **85**, 11A-0552.

[12] Watson, E.B. (1996) Surface Enrichment and Trace-Element Uptake during Crystal Growth. *Geochimica et Cosmochimica Acta*, **60**, 5013-5020. http://dx.doi.org/10.1016/S0016-7037(96)00299-2

[13] Watson, E.B. (2004) A Conceptual Model for Near-Surface Kinetic Controls on the Trace-Element and Stable Isotope Composition of Abiogenic Calcite Crystals. *Geochimica et Cosmochimica Acta*, **68**, 1473-1488. http://dx.doi.org/10.1016/j.gca.2003.10.003

[14] Watson, E.B. and Liang, Y. (1995) A Simple Model for Sector Zoning in Slowly Grown Crystals: Implications for Growth Rate and Lattice Diffusion, with Emphasis on Accessory Minerals in Crustal Rocks. *American Mineralogist*, **80**, 1179-1187.

[15] DePaolo, D.J. (2011) Surface Kinetic Model for Isotopic and Trace Element Fractionation during Precipitation of Calcite from Aqueous Solutions. *Geochimica et Cosmochimica Acta*, **75**, 1039-1056. http://dx.doi.org/10.1016/j.gca.2010.11.020

[16] Frisch, M.J., Trucks, G.W., Schlegel, H.B., Scuseria, G.E., Robb, M.A., Cheeseman, J.R., *et al.* (2009) Gaussian 09, Revision A.01. Gaussian, Inc., Wallingford.

[17] Rustad, J.R., Nelmes, S.L., Jackson, V.E. and Dixon, D.A. (2008) Quantum-Chemical Calculations of Carbon-Isotope Fractionation in $CO_2(g)$, Aqueous Carbonate Species, and Carbonate Minerals. *Journal of Physical Chemistry A*, **112**, 542-555. http://dx.doi.org/10.1021/jp076103m

[18] Kohn, W. and Sham, L.J. (1965) Self-Consistent Equations Including Exchange and Correlation Effects. *Physical Review*, **140**, A1133.

[19] Petersson, G.A. and Allaham, M.A. (1991) A Complete Basis Set Model Chemistry. II. Open-Shell Systems and the Total Energies of the First-Row Atoms. *Journal of Chemical Physics*, **94**, 6081-6090. http://dx.doi.org/10.1063/1.460447

[20] Petersson, G.A., Bennett, A., Tensfeldt, T.G., Allaham, M.A., Shirley, W.A. and Mantzaris, J. (1988) A Complete Basis Set Model Chemistry. I. The Total Energies of Closed-Shell Atoms and Hydrides of the First-Row Elements. *Journal of Chemical Physics*, **89**, 2193-2218. http://dx.doi.org/10.1063/1.455064

[21] Urey, H.C. (1947) The Thermodynamic Properties of Isotopic Substances. *Journal of the Chemical Society*, 562-581. http://dx.doi.org/10.1039/jr9470000562

[22] Bigeleisen, J. and Mayer, M.G. (1947) Calculation of Equilibrium Constants for Isotopic Exchange Reactions. *Journal of Chemical Physics*, **15**, 261-267. http://dx.doi.org/10.1063/1.1746492

[23] Jarosch, D. and Heger, G. (1986) Neutron Diffraction Refinement of the Crystal-Structure of Aragonite. *Tschermaks*

mineralogische und petrographische Mitteilungen, **35**, 127-131. http://dx.doi.org/10.1007/BF01140844

[24] Maslen, E.N., Streltsov, V.A. and Streltsova, N.R. (1993) X-Ray Study of the Electron-Density in Calcite, CaCo₃. *Acta Crystallographica Section B-Structural Science*, **49**, 636-641. http://dx.doi.org/10.1107/S0108768193002575

[25] Steinfink, H. and Sans, F.J. (1959) Refinement of the Crystal Structure of Dolomite. *American Mineralogist*, **44**, 679-682.

[26] Yuan, J. (2014) Reduced Partition Function Ratio in the Frequency Complex Plane: A Mathematical Approach. *Open Journal of Geology*, **4**, 654-664. http://dx.doi.org/10.4236/ojg.2014.412049

[27] Yuan, J. and Liu, Y. (2012) Quantum-Mechanical Equilibrium Isotopic Fractionation Correction to Radiocarbon Dating: A Theory Study. *Journal of Radioanalytical and Nuclear Chemistry*, **292**, 335-338. http://dx.doi.org/10.1007/s10967-011-1563-3

[28] Grauel, A.L., Schmid, T.W., Hu, B., Bergami, C., Capotondi, L., Zhou, L.P., *et al.* (2013) Calibration and Application of the "Clumped Isotope" Thermometer to Foraminifera for High-Resolution Climate Reconstructions. *Geochimica et Cosmochimica Acta*, **108**, 125-140. http://dx.doi.org/10.1016/j.gca.2012.12.049

[29] McCrea, J.M. (1950) On the Isotopic Chemistry of Carbonates and a Paleotemperature Scale. *Journal of Chemical Physics*, **18**, 849-857. http://dx.doi.org/10.1063/1.1747785

[30] Swart, P.K., Burns, S.J. and Leder, J.J. (1991) Fractionation of the Stable Isotopes of Oxygen and Carbon in Carbon-Dioxide during the Reaction of Calcite with Phosphoric-Acid as a Function of Temperature and Technique. *Chemical Geology*, **86**, 89-96.

[31] Cao, X. and Liu, Y. (2012) Theoretical Estimation of the Equilibrium Distribution of Clumped Isotopes in Nature. *Geochimica et Cosmochimica Acta*, **77**, 292-303. http://dx.doi.org/10.1016/j.gca.2011.11.021

[32] Wang, J., Qian, Z., Qian, W., Zhuang, Y., He, Y. and Pan, C. (1999) Probability Statistics (Engineering Mathematics). Tongji University, Shanghai, 240-247. (In Chinese)

[33] Cui, L.L. and Wang, X. (2014) Determination of Clumped Isotopes in Carbonate Using Isotope Ratio Mass Spectrometer: Effects of Extraction Potential and Long-Term Stability. *International Journal of Mass Spectrometry*, **372**, 46-50. http://dx.doi.org/10.1016/j.ijms.2014.08.006

[34] Levine, I.N. (1995) Physical Chemistry. 4th Edition, McGraw-Hill, Inc., New York.

Supplementary File

Optimized Geometries of Clusters in the Text

This file contains the optimized orientations of atoms in pure Ca^{2+}- and Mg^{2+}-dolomite clusters, shown in Figure 1; see geometries of pure aragonite and calcite in Yuan Jie, Zhang Zhigang, and Zhang Yigang (2014).

1. Ca-dolomite

```
C  -7.5733400   -23.8397780   -12.4229890
O  -7.4228400   -24.6390750   -11.4578180
O  -8.6174280   -23.9048960   -13.1449810
O  -6.6282910   -23.0460140   -12.7362840
C  -1.7264230   -25.2056520   -10.7438680
C  -3.6414910   -21.2804940   -11.4990970
C  -4.3212200   -24.2328130   -14.6843240
C  -4.9431820   -24.6966200   -8.2031210
C  -5.9471600   -27.4582630   -11.4057240
C  -6.1561990   -20.3564350   -15.7243240
C  -6.9657810   -23.2626220   -18.6000230
C  -8.6226660   -26.4099680   -15.3692490
C  -9.5033720   -26.6650300   -8.8632540
C  -10.2297630  -29.5680790   -12.0703700
C  -10.5070710  -22.5416530   -16.0910860
C  -12.1790360  -25.9898050   -12.8937390
Ca -4.9463600   -24.4090490   -11.4976160
Ca -7.4013510   -23.3752350   -15.2082180
Ca -8.9627020   -26.3811510   -12.1443530
O  -2.5298720   -20.7670240   -11.1672930
O  -4.1617190   -22.1788170   -10.7869430
O  -4.0543810   -23.8480350   -7.8761820
O  -1.1418760   -24.4256970   -11.5645050
O  -1.0918260   -25.6194470   -9.7274760
O  -2.9129110   -25.5630840   -10.9158060
O  -5.0657210   -25.6773190   -7.4110340
O  -4.9455340   -20.0130350   -15.8456260
O  -6.5487940   -21.1583260   -14.8497140
O  -4.2210580   -20.8723250   -12.5518890
O  -3.7353440   -23.4706660   -15.5199430
O  -3.7898220   -24.4261290   -13.5610240
O  -5.4276670   -24.7545070   -14.9814890
O  -5.6030050   -24.6170930   -9.2578540
O  -8.4091200   -26.1439850   -8.5164880
O  -5.3653060   -26.6878140   -12.2139000
O  -5.3315470   -27.8638010   -10.3671370
O  -7.1392280   -27.8224920   -11.5928840
O  -10.1031180  -27.4508950   -8.0631770
O  -6.9450740   -19.8771800   -16.5944150
O  -9.3407390   -22.1348030   -15.8504520
O  -6.3799010   -22.5216940   -19.4461160
O  -6.4716060   -23.3904490   -17.4540480
O  -8.0428030   -23.8482430   -18.9387610
O  -11.0940700  -23.3419960   -15.3061210
O  -11.0634900  -25.4299110   -12.7994790
O  -8.2069500   -25.4531850   -16.0751420
O  -8.0212430   -26.7502040   -14.3171290
O  -9.6838260   -27.0210230   -15.7174690
```

```
O  -12.7454750   -26.5523390   -11.9086590
O  -10.0106400   -26.4181360   -9.9906040
O  -9.8253590    -28.5923470   -12.7455960
O  -9.5998160    -29.9807600   -11.0445210
O  -11.2987220   -30.1609060   -12.4107820
O  -11.1031000   -22.1483490   -17.1413710
O  -12.7981400   -26.0950880   -13.9909140
O  -8.0522490    -23.1692160   -8.8474230
H  -8.9972600    -23.2340710   -8.7361220
H  -7.9597070    -22.6611450   -9.6463110
O  -7.3970110    -20.9334450   -10.7796960
H  -6.7366670    -21.4383370   -11.2427130
H  -7.0275540    -20.6363540   -9.9567440
O  -10.5714600   -22.0281150   -11.8777110
H  -10.3692450   -21.1047270   -12.0180460
H  -9.8639180    -22.5219310   -12.2827200
O  -9.5822110    -19.3100100   -11.7796700
H  -8.8498170    -19.7039800   -11.3097930
H  -9.1991060    -18.9273880   -12.5573870
O  -10.7909510   -22.3280240   -9.0814780
H  -10.7484240   -22.2110280   -10.0357180
H  -11.5619410   -22.8571190   -8.9285410
O  -8.5634340    -20.3079460   -8.0208860
H  -8.2273200    -21.1794000   -7.8435990
H  -9.4472280    -20.4771460   -8.3287230

2. Mg-dolomite
C  -7.6831990    -23.6286080   -12.3084500
O  -6.5985900    -22.9719120   -12.2668830
O  -8.4771140    -23.4934310   -13.2914400
O  -7.9793170    -24.4340290   -11.3738420
C  -5.0902760    -18.1037580   -12.7607900
C  -3.6345210    -21.2513710   -11.4931930
C  -6.6481970    -21.3144450   -9.5053430
C  -5.0004180    -24.7876210   -8.4554780
C  -8.2133780    -24.4535900   -6.1969590
C  -6.0590060    -20.6701160   -15.6601180
C  -9.2854610    -20.4253940   -13.4646460
C  -10.8694380   -23.5857400   -10.1159490
C  -9.2576800    -26.9936510   -9.0555940
C  -10.3610700   -22.9147740   -16.2918270
C  -13.5699700   -22.5597650   -14.0045180
C  -12.1135680   -25.6617460   -12.8333890
Mg    -6.3525950    -20.9741170   -12.5283720
Mg    -7.9444080    -24.1481000   -9.3880910
Mg    -10.5009900   -23.1841460   -13.1719360
O  -2.5149180    -20.7336170   -11.1846840
O  -4.1506450    -22.0921190   -10.7225150
O  -3.9521490    -24.1053060   -8.6481660
O  -5.0378150    -25.5928040   -7.4733360
O  -4.9820680    -20.0389300   -15.8924580
O  -5.0357330    -17.3311520   -13.7677380
O  -4.2060830    -18.0071630   -11.8574310
O  -6.0621750    -18.8822320   -12.6460140
```

```
O  -6.2328610   -21.3112760   -14.5982740
O  -4.2445850   -20.8940000   -12.5363630
O  -6.5609520   -20.5575800   -10.5014950
O  -5.8058710   -21.2086240   -8.5566870
O  -7.6347120   -22.0935710   -9.3994170
O  -5.9431440   -24.7178330   -9.2723880
O  -8.3180350   -26.1733490   -9.1118030
O  -7.9923260   -23.8558270   -7.2698390
O  -7.3686160   -24.3624760   -5.2536890
O  -9.2921570   -25.0900750   -5.9840100
O  -9.3051720   -27.8098650   -8.0832420
O  -6.9350990   -20.7109520   -16.5657340
O  -9.3147300   -22.2480170   -16.4914200
O  -9.2506310   -19.5600920   -14.3985690
O  -8.3857390   -20.4584670   -12.5909750
O  -10.2862500  -21.1771270   -13.3900890
O  -10.5545820  -23.5430700   -15.2204970
O  -10.9950750  -25.1322470   -12.6331450
O  -10.7444450  -22.8289180   -11.1105600
O  -9.9476770   -23.7093910   -9.2707270
O  -11.9764180  -24.1693070   -9.8856970
O  -12.6288020  -26.4761990   -12.0112390
O  -10.1332080  -27.0788460   -9.9688910
O  -11.2104110  -23.0163300   -17.2336820
O  -13.5235790  -21.7712750   -15.0051850
O  -12.6189910  -22.6234150   -13.1951490
O  -14.6380480  -23.2114160   -13.7891740
O  -12.7393670  -25.3793820   -13.8890490
O  -7.5264090   -25.1710230   -15.5013500
H  -7.8168010   -24.5696730   -14.8125000
H  -7.7709490   -26.0316500   -15.1869280
O  -7.1543270   -27.0978550   -12.0890710
H  -7.5779490   -26.3003260   -11.7742460
H  -6.2243280   -26.8875640   -12.0987070
O  -4.0515690   -23.8667690   -13.3608440
H  -4.9145670   -23.6072470   -13.0364350
H  -3.8979640   -24.7425180   -13.0182810
O  -6.3427200   -29.2530280   -13.7899360
H  -6.7480060   -28.6007190   -13.2219990
H  -7.0634620   -29.7022110   -14.2075540
O  -4.3446350   -26.7704320   -12.9999840
H  -4.5807710   -26.6414720   -13.9238680
H  -3.8837310   -27.5981420   -12.9714400
O  -4.6802200   -25.6608210   -15.5456550
H  -4.4786800   -24.8612340   -15.0627610
H  -5.5919550   -25.5511680   -15.8036420
```